Flexible Cellulose-Based Assembled with PEDOT: PSS Electrodes for ECG Monitoring

Yanping Wang
Donghua University - Songjiang Campus: Donghua University
Xing Zhong
Donghua University - Songjiang Campus: Donghua University
Wei Wang
Donghua University - Songjiang Campus: Donghua University
Dan Yu (yudan@dhu.edu.cn)
Donghua University Songjiang Campus https://orcid.org/0000-0003-4166-8026

Research Article

Keywords: Cotton fabric, Polyvinyl alcohol, PEDOT:PSS, Assembled, Flexible electrodes, ECG

Posted Date: March 23rd, 2021

DOI: https://doi.org/10.21203/rs.3.rs-207155/v1

Version of Record: A version of this preprint was published at Cellulose on March 31st, 2021. See the published version at https://doi.org/10.1007/s10570-021-03818-6.

Abstract

Electrocardiography is one of the most significant technologies for detecting cardiovascular diseases. Nowadays, the problems of various electrodes still meet a great challenge. Herein, we design a low cost, environmentally friendly and flexible conductive electrode using cellulose and polyvinyl alcohol as a substrate assembled with conductive polymer polythiophene by in-situ oxidative polymerization, and the green solvent 1-butyl-3-methylimidazolium chloride as a crosslinking agent. The polyvinyl alcohol/cellulose/PEDOT:PSS(PCPP) composite electrode has excellent features of flexibility, low skin contact impedance and comfortable contact with skin. When the load of EDOT reaches 15 wt%, the electrode is stable and can clearly monitor the characteristic wave of ECG signals. Therefore, based on cellulosic biopolymer and conductive polymer PEDOT:PSS, an environmentally friendly, flexible and stable PCPP composite electrode is obtained and can be a promising candidate applied in the fields of energy storage and ECG sensing.

1 Introduction

With the aging of the population and the prevalence of unhealthy lifestyles, cardiovascular and related diseases show an obvious growing trend nowadays(Akter Shathi et al. 2020a). Electrocardiogram (ECG) is one of the most important technologies for monitoring physiological function(Acar et al. 2019), based on the monitor many bioelectric signals containing important information of the human body, have been widely studied in medicine and scientific fields(Ankhili et al. 2018). By collecting the bioelectrical signals with electrodes on the surface of the body(Yamamoto et al. 2017), it is not only a clinical diagnosis of various heart diseases but also a simple and effective tool to explain arrhythmia and conduction disorders(Yapici and Alkhidir 2017). The mechanism of these electrodes is the depolarization and repolarization of myocardial cells will generate electric current. After this current is extracted, analyzed and processed by the instrument placed on the body surface, the dynamic curve of ECG signals can be obtained (Kaplan Berkaya et al. 2018). Obviously, the electrode is a very critical part of collecting bioelectric signals(Acar et al. 2019).

Electrodes mainly include wet electrodes, dry electrodes and flexible electrodes(Amale et al. 2018). The wet electrode mainly refers to the disposable electrode Ag/AgCl, which is a commercially available electrode at present. It has certain limitations that demand to be matched with a conductive gel to work properly. However, the conductive gel will cause allergic and other symptoms of the skin. Moreover, the gel will become dry in a short time, leading to the increase of noise and artifacts of the obtained electrical signals(Castrillón et al. 2018). Dry electrodes don’t need conductive gel(Puurtinen et al. 2006), but need to be firmly fixed on the skin with medical tape, which will also incur the uncomfortable feeling of the patients(Obukhov et al. 2012). Therefore, in order to meet the needs of long-term ECG acquisition, the design of a lightweight, flexible and highly sensitive electrode is extremely important(Shathi et al. 2020). Recent findings have shown that cellulose is a biocompatible and low-cost electrode substrate candidate(Akter Shathi et al. 2020b). Because of its excellent flexibility and mechanical stability, it has the potential to be regarded as structural support for wearable devices(Zhang et al. 2019; Zhang et al.

2020). When polythiophene(Zhao et al. 2017), polypyrrole(Abinaya and Muthuraj 2020; Chen et al. 2015; Jyothibasu and Lee 2020; Yang et al. 2020a), and polyaniline(Wang et al. 2019) are assembled with cellulose through strong interaction, to highly conductive flexible electrodes can be fabricated. For example, the introduction of conducting polymer poly (3,4-ethylene dioxythiophene): Polystyrene trans acid (PEDOT:PSS) can endow the electrodes with higher sensitivity to biological and chemical molecules, shorter response time, and realizes on-line real-time monitoring(Pani et al. 2016). A transparent and biocompatible strain sensor based on silver nanowires, regenerated cellulose film and PEDOT:PSS were prepared by coordination and hydrogen bonding(Xu et al. 2019). Using green solvents like ion liquid is a promising way to recycle cellulose from biomass (Rieland and Love 2020). Studies have found that 1-butyl-3-methylimidazolium hydrochloride is able to dissolve cellulose, realizing the recycling of cotton fabrics(Swatloski et al. 2002). After dissolution, a single cellulose macromolecular chain which could be further modified and self-assembled was obtained(Wang et al. 2012). As known to all, polyvinyl alcohol (PVA) has a large number of hydroxyl groups on the molecular chain with good biocompatibility, stability, and the built-in moisture content is comparable to human cell tissue(Huafeng and Shaopeng 2017). It can be combined with cellulose fibers due to the formation of hydrogen bonds between macromolecular chains (Sun et al. 2014). In particular, PVA can modify the stability of PEDOT:PSS electrode(Chen et al. 2011; Liu et al. 2011).

Therefore, in this paper, cotton fabric which is dissolved by the green solvent of 1-butyl-3-methylimidazolium chloride ([Bmim]Cl), is mixed with PVA turning into the substrate of a flexible electrode(Sellam and Hashmi 2013). Then PEDOT formed in the process of in-situ oxidation polymerizes with PSS to form polyvinyl alcohol/cellulose/PEDOT:PSS(PCPP) film electrode. This strategy may provide new ideas for the production of low cost, environmentally friendly conductive electrodes for ECG monitoring.

2. Experimental Section

2.1. Materials

In this experiment, cotton fabric was obtained from Shanghai San yuan Co. Ltd., sodium hydroxide (NaOH) was obtained from Ping Hu Chemical Reagent Factory, [Bmim]Cl was received from Shanghai Bidder Medical Technology Co. Ltd, EDOT and PSS were acquired from Shanghai Yi Shi Chemical Co. Ltd., ammonium persulfate (APS), ferric sulfate ($Fe_2(SO_4)_3$) and polyvinyl alcohol (PVA, a molecular weight of 88 kDa) were purchased from Sinopharm Group Chemical Reagent Co. Ltd.

All chemicals are analytical grade reagents and used without purification.

2.2. Pretreatment of cotton fabric

Cotton fabric was dipped into sodium hydroxide solution with a mass fraction of 2% for 2h at 80°C to remove impurities and grease on the fabric surface. Then it was rinsed by water at room temperature for

washing and soaking for a certain time. After filtering distilled water, the fabric was dried and sheared to pieces.

2.3. Preparation of the PVA/Cellulose/PEDOT:PSS (PCPP) films

[Bmim]Cl (3 g) was added to an eggplant shaped flask and heated at 100°C for 10 minutes. Then cotton fabric (3 wt% 0.09g) was added to the flask and mechanically stirred until a transparent and uniformly stable IL/cellulose system was received. Then PVA (1% 0.03g) was added into the mixture system. EDOT (0.3, 0.36, 0.45g) was dissolved in solution respectively to obtain IL/PVA/CEL/EDOT solution with different content of (10 wt%, 12 wt%, 15 wt%)EDOT, reacting 30min. The stirring rate of the reaction system needed to be reduced in order to allow IL/PVA/CEL/EDOT/ to perform an adequate cross-linking reaction. When the reaction was finished, keeping 30min under 100℃ to remove bubbles. The mixture solution was immediately cast into a Teflon mold while it was hot, and then the gel was cooled to room temperature, getting an IL/PVA/CEL/EDOT gel. Then the gel was soaked in distilled water, obtaining a white film. Polystyrene sulfonic acid (PSS) was used as a dopant; the film was then soaked in PSS solution at 35°C for 30 minutes. Ammonium persulfate (APS) and ferric sulfate ($Fe_2(SO_4)_3$) were added into the solution to initiate oxidative polymerization. The oxidation time was 12 h, and the color of the solution changes from clear to black. Then unreacted PSS was removed by washing with distilled water, obtaining a PVA/CEL/PEDOT:PSS hydrogel. The hydrogel was dried in a vacuum oven at 55°C for 8 hours to obtain a black PVA/CEL/PEDOT:PSS(PCPP) film.

2.4 Characterizations

2.4.1 Fourier transform infrared (FTIR) spectra

The FTIR spectra of Cellulose (CEL), PVA/CEL film, PVA/CEL/EDOT film, PVA/CEL/PEDOT:PSS samples were obtained from the FTIR system (FTIR, Nicolet 6700, USA) in the total reflection (ATR) attachment mode, and the frequency range was 400-4000 cm^{-1}.

2.4.2 Raman spectra

Raman imaging microscope (DXR2xi, Thermo Scientific, USA) was used to analyze the chemical structure of the samples. The laser beam length was 532 nm.

2.4.3 Scanning electron microscope (SEM)

The morphology of pure cellulose film, PVA/CEL film, PVA/CEL/EDOT film and PVA/CEL/PEDOT:PSS film were observed by scanning electron microscopy (SEM, TM-1000, Hitachi) Before testing, the samples were dried and then gold plated on the samples using a vacuum sputtering coater.

2.4.4 Conductivity testing

A four-point probe was used to measure the sheet resistance of the film. The water content in the conductive film would affect the test results. The film was pretreated in a constant temperature and humidity chamber for 24 h. The average resistance was calculated by taking 10 measured values, and the conductivity was calculated using the formula.

$$\sigma = {}^{1}/_{Rs * d} \qquad (1)$$

Rs is the sheet resistance of the film and d is the thickness of the film.

2.4.5 XPS spectra

X-ray photoelectron spectroscopy (XPS) was used to detect the surface element composition and atomic valence state of 15 wt% PCPP film in the range of 0-1200ev.

2.4.6 Electrochemical Measurements

CV and EIS were studied by CHI 660E electrochemical analyzer (CHI 660E, Chen Hua, China). The CV scan data were obtained in a 1.0 V voltage window, using simulated sweat as the electrolyte, and the scan rate was 0.01-0.09V/s. The EIS measurement was performed in the frequency range of 0.01 Hz to 100 kHz.

2.4.7 ECG measurements

A standard □-lead ECG measurement was performed using 15 wt% PCPP film electrodes to evaluate the bio-signal sensing performance. The electrodes are connected to the left and right wrists of the volunteer's body and then connected to a commercial ECG device (BDM101) through lead wires to record ECG signals. The digital signal is transmitted to the PC or mobile phone through the amplifier and ADC converter.

3. Results And Discussion

3.1 Design and synthesis of the PVA/CEL/PEDOT:PSS(PCPP) films

Figure1a shows the process of obtaining PVA/CEL/PEDOT:PSS conductive film. Cellulose was cross-linked with PVA, forming a flexible template to guide the in-situ polymerization of EDOT along the polymer chain. Firstly, the pretreated waste cotton fabric was dissolved into a single cellulose macromolecular chain in the [Bmim]Cl system. At the beginning of dissolution, the fibers with linear and micron-level can be clearly seen under the optical microscope, which was orderly arranged and had uniform thickness. After a period of dissolution treatment, the existence of cellulose can not be observed under the magnification of 100 times, indicating that cellulose was completely dissolved (Fig. 1b). After that, PVA was added into the homogeneous and transparent solution of IL/CEL, and cross-linked with

cellulose through hydrogen bonding to obtain a network structure, which provided a favorable flexible template for the oxidative polymerization of EDOT(Zhao et al. 2017). The solution was cast into a mold while it was hot, and a white PVA/CEL/EDOT(PCE) film was obtained after cooling and solidification. This film was obtained after water exchanged the IL solvent. EDOT was oxidized and polymerized along the flexible polymer chain in the environment of PSS as dopant, ammonium persulfate and ferric sulfate as oxidant. In the process of doping, PEDOT may be attached to one PSS chain or more PSS chains, and gradually cross-linked to form particles with strong force(Kirchmeyer and Reuter 2005). During the oxidation process, the white gel film gradually turns black over time (Fig. 1c, d). After drying, a black flexible PCPP film was obtained which can be curled and folded. In the reaction process, the amount of EDOT played a decisive role, which determined the conductivity of PCPP film. If the quantity of EDOT is insufficient, the conductivity of PCPP film is uneven. As the addition of EDOT (Figure S1), the accumulation of it was taken place and the optimum amount of EDOT should be selected as 15 wt%.

3.2 Chemical Structure and Morphology of the Composite Films

Figure 2 showed the infrared spectrum and Raman spectrum of the sample. As shown in the infrared spectrum (Fig. 2a), the peaks at 844cm^{-1}, 793cm^{-1} and 694cm^{-1} on PVA/CEL/EDOT (PCE) film are assigned to the bending vibration absorption peaks of C = C-H in EDOT thiophene ring(Zhou et al. 2011). After oxidative polymerization, the three peaks disappear as shown by the peak on PCPP film, which indicates that EDOT is oxidative polymerized and PEDOT is connected by α-α'(Zubair et al. 2016). The absorption vibration peaks of C-O-C in EDOT are 1261cm^{-1} and the surrounding peaks, which deform after polymerization(Xu et al. 2010). The new peak of 1526 cm^{-1} on PCPP film is related to the absorption peak of an oxygen-containing matrix in PEDOT(Kwon et al. 2010). The peaks appearing at 1029 cm^{-1} for the four samples belong to the C-O stretching vibration peak in the CEL substrate structure. After EDOT is oxidized to PEDOT, peak here on PCPP film becomes significantly weaker, which may be the oxidative polymerization of EDOT along cellulose macromolecular chain(Ziyang et al. 2020). The peak at 1640 cm^{-1} is the vibration absorption peak of H-O-H(Yang et al. 2020b). The peak of the PCPP film becomes stronger here, indicating that PVA/CEL/PEDOT interact through intramolecular or intermolecular hydrogen bonding. It can be seen from the Raman spectrum(Fig. 2b) that 438 cm^{-1}, 570 cm^{-1}, 984 cm^{-1}, 1255 cm^{-1} and 1424 cm^{-1} peaks belong to the C-O-C deformation peak of PEDOT, the symmetrical C-S-C deformation peak, the ring deformation peak of oxyacetylene(Nur Afifah et al. 2016), and the stretching deformation of Cα-Cα inner ring, and the symmetric stretching deformation of Cα-Cβ, respectively(Jian et al. 2018). The characteristic peak intensity in the range of 2500 cm^{-1} to 3000 cm^{-1} is regarded as the characteristic peak intensity of PVA, and the stretching vibration excitation of methylene (-CH_2) occurs at 2840 cm^{-1}(Li et al. 2020).

From the XPS survey spectrum of 15 wt% PCPP film (Fig. 3), C1s, O1s and S2p numbers can be clearly seen, which indicates that PEDOT:PSS successfully bonded to the cellulose/PVA matrix film. The

existence of C, O and S elements is further confirmed by energy spectrum analysis (Figure S2). The high-resolution C1s spectra of 15wt % PCPP film showed five different peaks (Fig. 3b). The peak generated at 284.71 eV is attributed to C = C in the aromatic structure of PEDOT, and the aliphatic C-C peak of the PSS chain is generated at 284.81 eV. The peak at 286.10 eV corresponds to the chemical environment of C element in the C-O/C-S structure. The peak at 286.40 eV generally refers to the C-O in the polyvinyl alcohol. Two main peaks are observed in the S 2p spectrum (Fig. 3c)(Guo et al. 2013). The two low binding energy peaks at 163.71 eV and 164.84 eV are attributed to the S atom in PEDOT(Zahed et al. 2020), while the two high binding energy peaks at 168.81 eV and 168.27 eV are due to the interaction of neutral S atoms and S ions in PSS(Merche et al. 2010). The two main peaks of the PEDOT and PSS chains indicate that PSS was successfully doped into the PVA/CEL/EDOT film structure and had a strong π-π interaction with PEDOT during the oxidation process. The 532.34 eV and 532.11 eV shown in the O 1s spectrum (Fig. 3d) are homogeneously dispersed to the PEDOT and PSS.

The SEM images show the surface morphology of the samples (Fig. 4). The comparison between Fig. 4a and Fig. 4b shows that the surface of cellulose film is rough, and the addition of PVA makes the film surface smooth. This may be due to the large number of hydroxyl groups in the molecular chain of PVA and cellulose that cross-link with each other to form hydrogen bonds, optimizing the morphology of the film. As shown in the image of the PCE film (Fig. 4c), EDOT particles are deposited on the structure of the film. After in-situ polymerization and oxidation, pores of different degrees appear on the surface of 10 wt%, 12 wt% and 15 wt% PCPP films (Fig. 4d-f). On one side, it may be caused by a solvent exchange of ionic liquids in the coagulation bath, the other side of the shield, it is speculated that it is caused by PSS doping. The number of pores distributed on 10 wt% PCPP film is much less than that of 15 wt% film. In addition, the pore distribution on the 15 wt% PCPP film was uniform. From the statistical distribution of the average diameter of 15 wt% PCPP film (Fig. 4f´), it can be clearly observed that the average pore diameter is mainly 8 μm. However, large pores are easier to collapse. When water is used as a solvent to exchange ionic liquids, it will have a significant impact on the morphology of the cellulose film. According to the existing research(Khare et al. 2007; Liu and Budtova 2012; Swatloski et al. 2002), when ethanol is used as a coagulation bath, the film with smaller pore size and denser pore distribution can be obtained. To avoid the problem of macroporous defects, it is necessary to carry out experimental exploration. When the cellulose, PVA and (10 wt%, 12 wt% and 15 wt%) EDOT were dissolved in the ionic liquid to form a uniform and transparent solution, and it was cooled and solidified in the mold, the next step was to use ethanol as coagulation bath instead of deionized water to precipitate the ionic liquid. The other steps were unchanged. After drying, the surface morphology of PCPP films was observed by SEM. As shown in Fig. 4 (g-i), the pore size on the surface of the PCPP films reaches a few microns with a uniform pore distribution. At the same time, the sheet resistances of PCPP films were measured by a four-point probe, and it is found that the resistance decreases slightly, but the overall trend does not change (Figure S5). Correspondingly, ECG monitoring was performed, and there was no difference between the ECG signal spectra obtained by the original method.

It can be seen from the test results of mechanical properties (Fig. 5a), in the cellulose/PVA composite film, the addition of PVA can improve the tensile strength of the membrane. The increase of mechanical

properties is attributed to the interaction between cellulose and PVA, especially the hydrogen bond. When EDOT is added and oxidized, the tensile strength of PCPP films decreases greatly. It can be speculated that oxidants (APS and Fe^{3+}) will reduce the mechanical properties of PCPP films. The tensile strength of the three groups of PCPP films has no obvious difference. The outstanding one is that the elongation at break of 15% PCPP film is the highest, and the stronger the tear resistance, the better the flexibility and elasticity. The electrode is the interface between the human body and the bioelectric collection device. The current in the biological body in the form of ions is converted into the electronic current in the collection device through the electrode(Lee et al. 2020). Therefore, the conductivity of the electrode will affect the accuracy of ECG signal transmission. The sheet resistance value of 10 wt% PCPP film is 5.543 $k\Omega \cdot sq^{-1}$, the sheet resistance value of 12 wt% PCPP film is 3.201 $k\Omega \cdot sq^{-1}$, and the sheet resistance value of 15 wt% PCPP film is 0.196 $k\Omega \cdot sq^{-1}$ (Fig. 5b). The curled state has no obvious influence on the resistance value. The sheet resistance of the film electrodes increased with the increase of the EDOT loading, and the 15 wt% PCPP film showed the optimum conductivity because EDOT was evenly dispersed into the network structure of PVA/CEL, when its addition amount reached 15 wt%. Because of the evaporation of water, the resistance of the PCPP films increased to some extent with time. Compared with the first day, the resistance increased significantly on the seventh day (Fig. 5c).

The electrochemical tests were carried out to exhibit the reaction process between the skin and the electrode film. Sweat is inevitable on the surface of human skin, so when measuring ECG signals, film electrode and sweat constitute an electrochemical system, in which film electrode reacts as working electrode and sweat acts as an electrolyte. In order to simulate the reaction process between ECG electrode and skin as much as possible, the electrolyte is simulated sweat. The components of simulated sweat are 20g/L sodium chloride and 1g/L urea. Cyclic voltammetry curve and EIS impedance curve were obtained. Figure 5d shows the test results of cyclic voltammetry curves of different samples at 0.01 Vs^{-1}. The three curves all conform to the CV shape of the polymer as the electrode material. Compared with the CV curve area of 10 wt% PCPP, 12 wt% PCPP, 15 wt% PCPP film at a scanning rate of 0.01V/s, the larger the area enclosed by the curve, the more conducive to the charge and discharge reaction, which means the better the redox performance. The area of the 15 wt% PCPP film is obviously the largest, and the curve is close to a symmetrical rectangle. Redox peaks generate belonging to the energy storage mechanism of pseudocapacitance, which further proves the existence of PEDOT in the composite film. The curve area of 12 wt% PCPP is roughly half of that of 15 wt% PCPP electrode, and the area of 10 wt% sample is the smallest, which shows that with the increase of EDOT concentration, the performance of the PCPP electrode is better. Then three samples were tested by cyclic voltammetry at different scanning speeds (Fig. 6a-c). The redox peaks are observed from the CV curves of 10 wt% PCPP film. This is because the conductive polymer PEDOT generates capacitance through redox reactions, and the energy storage it produces throughout the material, not just on the surface(Anton et al. 2017). EIS impedance diagram was used to test the electron transfer performance of PCPP film(Priniotakis et al. 2007) and the EIS of 10 wt% PCPP film with electron transfer resistance tended to a straight line in both high and low-frequency regions(Fig. 6d), indicating that the electrode reaction was not affected by electron transfer restriction, but controlled by the diffusion process. Small semicircles appeared in the high-frequency region of EIS

(Fig. 6e, f), which indicated that there was charge transfer resistance between the electrode and the skin surface. The charge transfer resistance at the interface of 15 wt% PCPP was significantly lower than that of 12 wt% PCPP film, which could be attributed to the dense structure formed by the uniform dispersion of PEDOT on the 15 wt% PCPP film. In addition, the porous structure of the PCPP film surface provides a large surface area and a large number of active sites on the electrode surface. The cross-linked structure of PVA/CEL through hydrogen bonding makes the conductive path more succession and uninterrupted, resulting in faster electron transfer and higher conductivity(Nur Afifah et al. 2016).

3.3 Performance of PCPP film Electrodes in ECG Monitoring

The equipment for ECG signal acquisition is a commercial BMD101 ECG(Ai et al. 2018) development module (Fig. 7a). The main components of the analog front-end include a low-noise amplifier and analog-to-digital(A/D)converter ADC(Rashkovska et al. 2020), which can digitally process the analog signal (Fig. 7b), and the data value can be transmitted to PC or mobile phone through the standard Bluetooth serial port Pro Le (SPP). The acquired signal is processed by MATLAB (R 2018a). The BMD101 ECG acquisition device comes with two lead wires lead I so the PCPP film electrodes are connected to the wrists of the left and right hands(Lo et al. 2018), using the standard lead I, and the ECG signals of two volunteers at rest are collected. ECG signals were collected by PCPP film electrode, and the acquired data is filtered by MATLAB to obtain the ECG signal spectrogram. A normal ECG signal is composed of a series of wave groups, including P wave, QRS wave, and T wave. The p wave represents the depolarization of the atrium, the QRS wave corresponds to the depolarization wave of the ventricle, and the T wave represents the repolarization wave of the ventricle. The ECG spectrum obtained by 10 wt% PCPP film electrode showed a regular signal value, but the PQRST characteristic wave was not detected, which is closely related to the insufficient load of EDOT in the 10 wt% film electrode and the high sheet resistance. On the ECG spectrum obtained by 12 wt% film electrode, there are still many obvious noises after processing, but the existence of Q and R waves can be clearly observed (Fig. 7d). Interestingly, these waves could be clearly detected from the ECG spectra of two volunteers using the 15 wt% film electrode (Fig. 7e, f). After 7 days, the ECG signal spectrum detected by 15 wt% PCPP film electrode showed more noise, compared with 10 wt% and 12 wt% ECG, QRS wave could still be detected, which indicated that the conductivity of ECG film electrode played an important role in the detection of ECG signals. The ECG signals obtained by 10 wt% and 12 wt% PCPP film electrodes are unstable, with a lot of noise and too much chance, causing poor characteristic waves. Compared to others, the performance of 15 wt% PCPP film electrode is more stable, which is due to the excellent conductivity of PEDOT and the stable structure assembled by EDOT and PVA /CEL in 15 wt% PCPP film.

4. Conclusions

In this work, a flexible cellulose-based assembly with PEDOT:PSS composite electrode was prepared to monitor the ECG signals. The conductivity of PCPP film can be optimized by controlling the content of

EDOT. When the addition of EDOT reaches 15 wt%, the sheet resistance value of PCPP film decreases sharply, compared with that of 10%, 12% PCPP film. Stable electrode performance can be maintained even in a crimped state. The characteristic wave of the ECG signal obtained through the 15 wt% PCPP film is clear. During the signal measurement, no skin irritation was observed, and because of the excellent flexibility of PCPP film, it is more comfortable to wear. We believe that conductive composite materials based on cellulose biopolymer and conductive polymer PEDOT:PSS show a bright future in the fields of energy storage and electrical signal sensing.

Declarations

Conflicts of interest

There are no conflicts to declare.

Acknowledgment

The present work was supported by “the Fundamental Research Funds for the Central Universities” (No. 2232020G-04).

References

Abinaya M, Muthuraj V (2020) Bi-functional catalytic performance of silver manganite/polypyrrole nanocomposite for electrocatalytic sensing and photocatalytic degradation Colloids and Surfaces A: Physicochemical and Engineering Aspects 604:125321 doi:https://doi.org/10.1016/j.colsurfa.2020.125321

Acar G, Ozturk O, Golparvar AJ, Elboshra TA, Böhringer K, Yapici MK (2019) Wearable and Flexible Textile Electrodes for Biopotential Signal Monitoring: A review Electronics 8 doi:10.3390/electronics8050479

Ai Z, Zheng L, Qi H, Cui W Low-Power Wireless Wearable ECG Monitoring System Based on BMD101. In: 2018 37th Chinese Control Conference (CCC), 25-27 July 2018 2018. pp 7374-7379. doi:10.23919/ChiCC.2018.8484125

Akter Shathi M, Minzhi C, Khoso NA, Deb H, Ahmed A, Sai Sai W (2020a) All organic graphene oxide and Poly (3, 4-ethylene dioxythiophene) - Poly (styrene sulfonate) coated knitted textile fabrics for wearable electrocardiography (ECG) monitoring Synthetic Metals 263:116329 doi:https://doi.org/10.1016/j.synthmet.2020.116329

Akter Shathi M, Minzhi C, Khoso NA, Deb H, Ahmed A, Sai Sai W (2020b) All organic graphene oxide and Poly (3, 4-ethylene dioxythiophene) - Poly (styrene sulfonate) coated knitted textile fabrics for

wearable electrocardiography (ECG) monitoring Synthetic Metals 263 doi:10.1016/j.synthmet.2020.116329

Amale A, Xuyuan T, Cédric C, Vladan K, David C, Jean-Michel T (2018) Comparative Study on Conductive Knitted Fabric Electrodes for Long-Term Electrocardiography Monitoring: Silver-Plated and PEDOT:PSS Coated Fabrics Sensors doi:10.3390/s18113890

Ankhili A, Tao X, Cochrane C, Coulon D, Koncar V (2018) Washable and Reliable Textile Electrodes Embedded into Underwear Fabric for Electrocardiography (ECG) Monitoring Materials 11 doi:10.3390/ma11020256

Anton VV et al. (2017) Understanding the Capacitance of PEDOT:PSS Advanced Functional Materials doi:10.1002/adfm.201700329

Castrillón R, Pérez JJ, Andrade-Caicedo H (2018) Electrical performance of PEDOT:PSS-based textile electrodes for wearable ECG monitoring: a comparative study BioMedical Engineering OnLine 17:38 doi:10.1186/s12938-018-0469-5

Chen C-h, Torrents A, Kulinsky L, Nelson RD, Madou MJ, Valdevit L, LaRue JC (2011) Mechanical characterizations of cast Poly(3,4-ethylene dioxythiophene): Poly(styrene sulfonate)/Polyvinyl Alcohol thin films Synthetic Metals 161:2259-2267 doi:https://doi.org/10.1016/j.synthmet.2011.08.031

Chen J, Xu J, Wang K, Qian X, Sun R (2015) Highly Thermostable, Flexible, and Conductive Films Prepared from Cellulose, Graphite, and Polypyrrole Nanoparticles ACS Applied Materials & Interfaces 7:15641-15648 doi:10.1021/acsami.5b04462

Guo X, Jian J, Lin L, Zhu H, Zhu S (2013) O2 plasma-functionalized SWCNTs and PEDOT/PSS composite film assembled by dielectrophoresis for ultrasensitive trimethylamine gas sensor Analyst 138:5265-5273 doi:10.1039/C3AN36690A

Huafeng P, Shaopeng W Properties and Reinforcing Mechanism of Cellulose Reinforced Polyvinyl Alcohol Hydrogel Membranes. In: International Symposium on Mechanical Engineering and Material Science (ISMEMS 2017), 2017/11 2017. Atlantis Press, pp 25-28. doi:https://doi.org/10.2991/ismems-17.2018.6

Jian H et al. (2018) A General Method for High-Performance Li-Ion Battery Ge Composites Electrodes from Ionic Liquid Electrodeposition without Binders or Conductive Agents: the Cases of CNTs, RGO and PEDOT Chemical Engineering Journal

Jyothibasu JP, Lee R-H (2020) Green synthesis of polypyrrole tubes using curcumin template for excellent electrochemical performance in supercapacitors Journal of Materials Chemistry A 8:3186-3202 doi:10.1039/C9TA11934E

Kaplan Berkaya S, Uysal AK, Sora Gunal E, Ergin S, Gunal S, Gulmezoglu MB (2018) A survey on ECG analysis Biomedical Signal Processing and Control 43:216-235 doi:https://doi.org/10.1016/j.bspc.2018.03.003

Khare VP, Greenberg AR, Kelley SS, Pilath H, Juhn Roh I, Tyber J (2007) Synthesis and characterization of dense and porous cellulose films Journal of Applied Polymer Science 105:1228-1236 doi:https://doi.org/10.1002/app.25888

Kirchmeyer S, Reuter K (2005) Scientific importance, properties and growing applications of poly(3,4-ethylene dioxythiophene) Journal of Materials Chemistry 15:2077-2088 doi:10.1039/B417803N

Kwon OS, Park E, Kweon OY, Park SJ, Jang J (2010) Novel flexible chemical gas sensor based on poly(3,4-ethylene dioxythiophene) nanotube membrane Talanta 82:1338-1343 doi:10.1016/j.talanta.2010.06.058

Lee Y et al. (2020) Self-Adherent Biodegradable Gelatin-Based Hydrogel Electrodes for Electrocardiography Monitoring Sensors 20 doi:10.3390/s20205737

Li W et al. (2020) Ionic Liquids Grafted Cellulose Nanocrystals for High-Strength and Toughness PVA Nanocomposite ACS Applied Materials & Interfaces doi:10.1021/acsami.0c11217

Liu N, Fang G, Wan J, Zhou H, Long H, Zhao X (2011) Electrospun PEDOT:PSS-PVA nanofiber-based ultrahigh-strain sensors with controllable electrical conductivity J Mater Chem 21:18962-18966 doi:10.1039/C1JM14491J

Liu W, Budtova T (2012) Ionic liquid: A powerful solvent for homogeneous starch-cellulose mixing and making films with tuned morphology Polymer 53:5779-5787 doi:https://doi.org/10.1016/j.polymer.2012.10.043

Lo C-I et al. (2018) Evaluation of the Accuracy of ECG Captured by CardioChip through Comparison of Lead I Recording to a Standard 12-Lead ECG Recording Device Acta Cardiol Sin 34:144-151 doi:10.6515/ACS.201803_34(2).20170919A

Merche D, Hubert J, Poleunis C, Yunus S, Bertrand P, De Keyzer P, Reniers F (2010) One Step Polymerization of Sulfonated Polystyrene Films in a Dielectric Barrier Discharge Plasma Processes and Polymers 7:836-845 doi:https://doi.org/10.1002/ppap.201000024

Nur Afifah Z, Norizah Abdul R, Hong Ngee L, Ruzniza Mohd Z, Yusran S (2016) Electrochemical properties of PVA–GO/PEDOT nanofibers prepared using electrospinning and electropolymerization techniques RSC Advances doi:10.1039/c5ra21230h

Obukhov AG, Tsukada S, Nakashima H, Torimitsu K (2012) Conductive Polymer Combined Silk Fiber Bundle for Bioelectrical Signal Recording PLoS ONE 7 doi:10.1371/journal.pone.0033689

Pani D, Dessi A, Saenz-Cogollo JF, Barabino G, Fraboni B, Bonfiglio A (2016) Fully Textile, PEDOT:PSS Based Electrodes for Wearable ECG Monitoring Systems IEEE Trans Biomed Eng 63:540-549 doi:10.1109/TBME.2015.2465936

Priniotakis G, Westbroek P, Van Langenhove L, Hertleer C (2007) Electrochemical impedance spectroscopy as an objective method for characterization of textile electrodes Transactions of the Institute of Measurement and Control 29:271-281 doi:10.1177/0142331207081605

Puurtinen MM, Komulainen SM, Kauppinen PK, Malmivuo JAV, Hyttinen JAK Measurement of noise and impedance of dry and wet textile electrodes, and textile electrodes with hydrogel. In: 2006 International Conference of the IEEE Engineering in Medicine and Biology Society, 30 Aug.-3 Sept. 2006 2006. pp 6012-6015. doi:10.1109/IEMBS.2006.260155

Rashkovska A, Depolli M, Tomašić I, Avbelj V, Trobec R (2020) Medical-Grade ECG Sensor for Long-Term Monitoring Sensors 20 doi:10.3390/s20061695

Rieland JM, Love BJ (2020) Ionic liquids: A milestone on the pathway to greener recycling of cellulose from biomass Resources, Conservation and Recycling 155:104678 doi:https://doi.org/10.1016/j.resconrec.2019.104678

Sellam, Hashmi SA (2013) High Rate Performance of Flexible Pseudocapacitors fabricated using Ionic-Liquid-Based Proton Conducting Polymer Electrolyte with Poly(3, 4-ethylene dioxythiophene): Poly(styrene sulfonate) and Its Hydrous Ruthenium Oxide Composite Electrodes ACS Applied Materials & Interfaces doi:10.1021/am4005557

Shathi MA, Chen M, Khoso NA, Rahman MT, Bhattacharjee B (2020) Graphene coated textile-based highly flexible and washable sports bra for human health monitoring Materials & Design 193:108792 doi:https://doi.org/10.1016/j.matdes.2020.108792

Sun X, Lu C, Liu Y, Zhang W, Zhang X (2014) Melt-processed poly(vinyl alcohol) composites filled with microcrystalline cellulose from waste cotton fabrics Carbohydrate Polymers 101:642-649 doi:https://doi.org/10.1016/j.carbpol.2013.09.088

Swatloski RP, Spear SK, Holbrey JD, Rogers RD (2002) Dissolution of Cellulose with Ionic Liquids Journal of the American Chemical Society 124:4974-4975 doi:10.1021/ja025790m

Wang D-C et al. (2019) Supramolecular Self-Assembly of 3D Conductive Cellulose Nanofiber Aerogels for Flexible Supercapacitors and Ultrasensitive Sensors ACS Applied Materials & Interfaces 11:24435-24446 doi:10.1021/acsami.9b06527

Wang H, Gurau G, Rogers RD (2012) Ionic liquid processing of cellulose Chemical Society Reviews 41:1519-1537 doi:10.1039/C2CS15311D

Xu Q, Li Y, Feng W, Yuan X (2010) Fabrication and electrochemical properties of polyvinyl alcohol/poly(3,4-ethylene dioxythiophene) ultrafine fibers via electrospinning of EDOT monomers with subsequent in situ polymerization Synthetic Metals 160:88-93 doi:10.1016/j.synthmet.2009.10.010

Xu W, Jianhong Z, Ying Z, Wanke C, Dawei Z, Guangwen X, Haipeng Y (2019) Assembly of silver nanowires and PEDOT:PSS with hydro cellulose toward highly flexible, transparent and conductivity-stable conductors Chemical Engineering Journal doi:10.1016/j.cej.2019.123644

Yamamoto Y, Yamamoto D, Takada M, Naito H, Arie T, Akita S, Takei K (2017) Efficient Skin Temperature Sensor and Stable Gel-Less Sticky ECG Sensor for a Wearable Flexible Healthcare Patch Advanced Healthcare Materials 6 doi:10.1002/adhm.201700495

Yang C et al. (2020a) Highly Conductive, Stretchable, Adhesive, and Self-Healing Polymer Hydrogels for Strain and Pressure Sensor Macromolecular Materials and Engineering 305:2000479 doi:https://doi.org/10.1002/mame.202000479

Yang M, Zhang X, Guan S, Dou Y, Gao X (2020b) Preparation of lignin-containing cellulose nanofibers and its application in PVA nanocomposite films International Journal of Biological Macromolecules 158:1259-1267 doi:https://doi.org/10.1016/j.ijbiomac.2020.05.044

Yapici MK, Alkhidir TE (2017) Intelligent Medical Garments with Graphene-Functionalized Smart-Cloth ECG Sensors Sensors 17 doi:10.3390/s17040875

Zahed MA, Das PS, Maharjan P, Barman SC, Sharifuzzaman M, Yoon SH, Park JY (2020) Flexible and robust dry electrodes based on electroconductive polymer spray-coated 3D porous graphene for long-term electrocardiogram signal monitoring system Carbon 165:26-36 doi:10.1016/j.carbon.2020.04.031

Zhang K, Tao P, Zhang Y, Liao X, Nie S (2019) Highly thermal conductivity of CNF/AlN hybrid films for thermal management of flexible energy storage devices Carbohydrate Polymers 213:228-235 doi:https://doi.org/10.1016/j.carbpol.2019.02.087

Zhang Y, Hao N, Lin X, Nie S (2020) Emerging challenges in the thermal management of cellulose nanofibril-based supercapacitors, lithium-ion batteries and solar cells: A review Carbohydrate Polymers 234:115888 doi:https://doi.org/10.1016/j.carbpol.2020.115888

Zhao D et al. (2017) Highly Flexible and Conductive Cellulose-Mediated PEDOT:PSS/MWCNT Composite Films for Supercapacitor Electrodes ACS Applied Materials & Interfaces 9:13213-13222 doi:10.1021/acsami.7b01852

Zhou W, Hu X, Bai X, Zhou S, Sun C, Yan J, Chen P (2011) Synthesis and Electromagnetic, Microwave Absorbing Properties of Core-Shell Fe_3O_4–Poly(3, 4-ethylene dioxythiophene) Microspheres ACS

Applied Materials & Interfaces 3:3839-3845 doi:10.1021/am2004812

Ziyang C, Xianhui A, Xueren Q (2020) Boosting electrical properties of flexible PEDOT/cellulose fiber composites through the enhanced interface connection with novel combined small-sized anions Cellulose doi:10.1007/s10570-019-02958-0

Zubair NA, Rahman NA, Lim HN, Zawawi RM, Sulaiman Y (2016) Electrochemical properties of PVA-GO/PEDOT nanofibers prepared using electrospinning and electropolymerization techniques RSC Advances 6:17720-17727 doi:10.1039/C5RA21230H

Figures

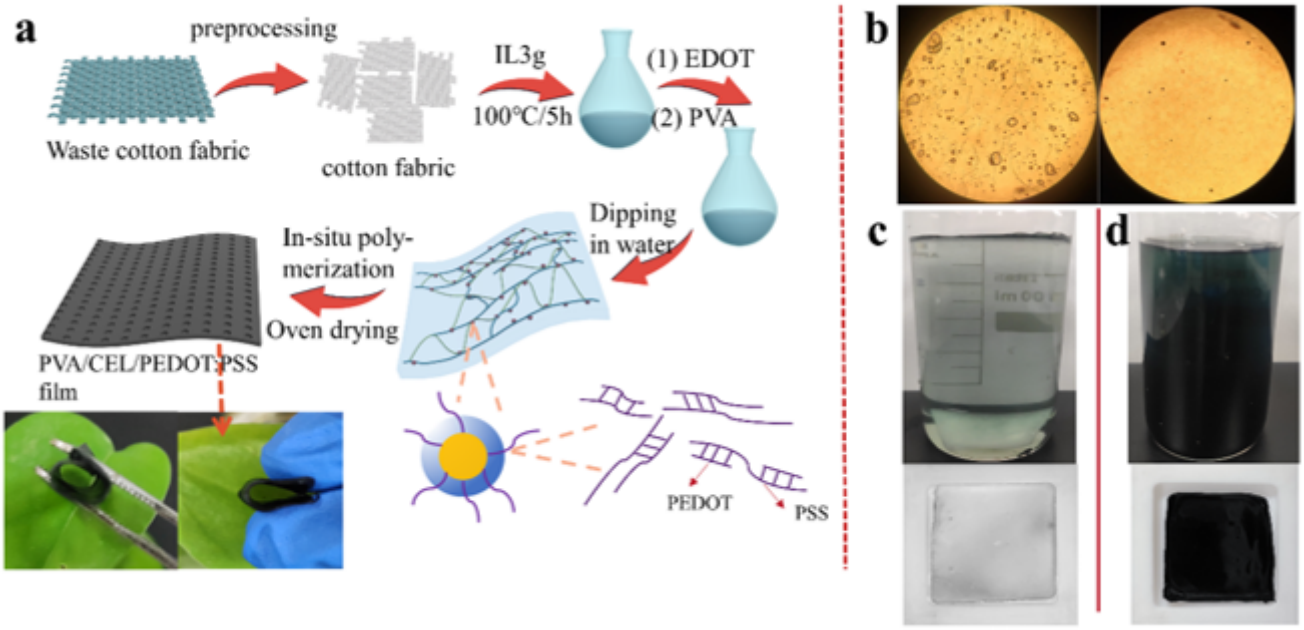

Figure 1

(a)Schematic presentation of the preparation procedure for PCPP films. (b)Before and after cellulose dissolution under an optical microscope magnification of 100 times. (c) Solution and PCE film before oxidation. (d) Solution and PCPP film after oxidation

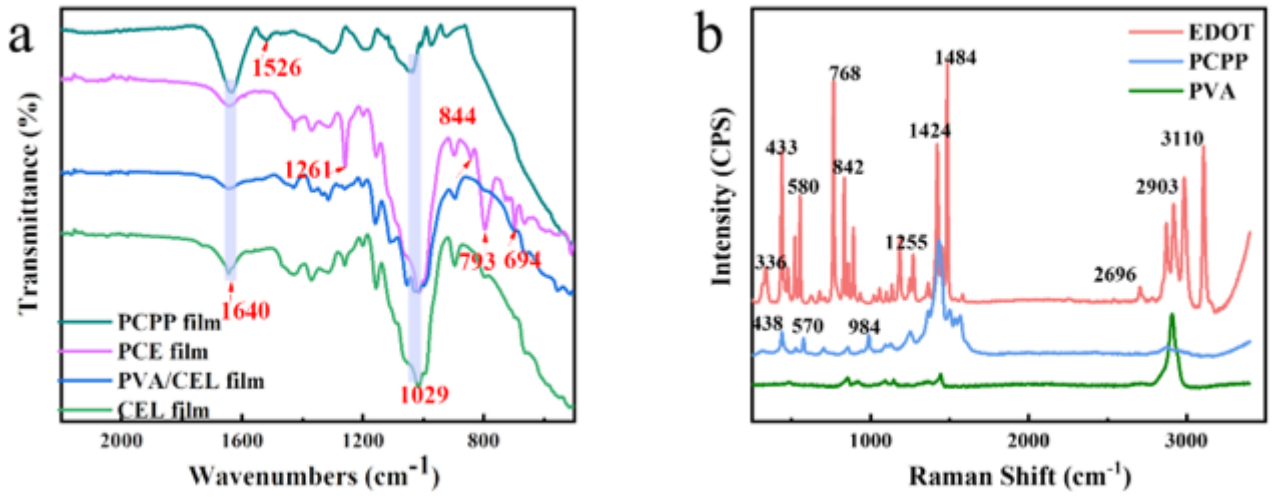

Figure 2

(a)FTIR spectra of CEL, PVA/CEL, PCE, PCPP film. (b)Raman spectra of PVA, PCPP, EDOT.

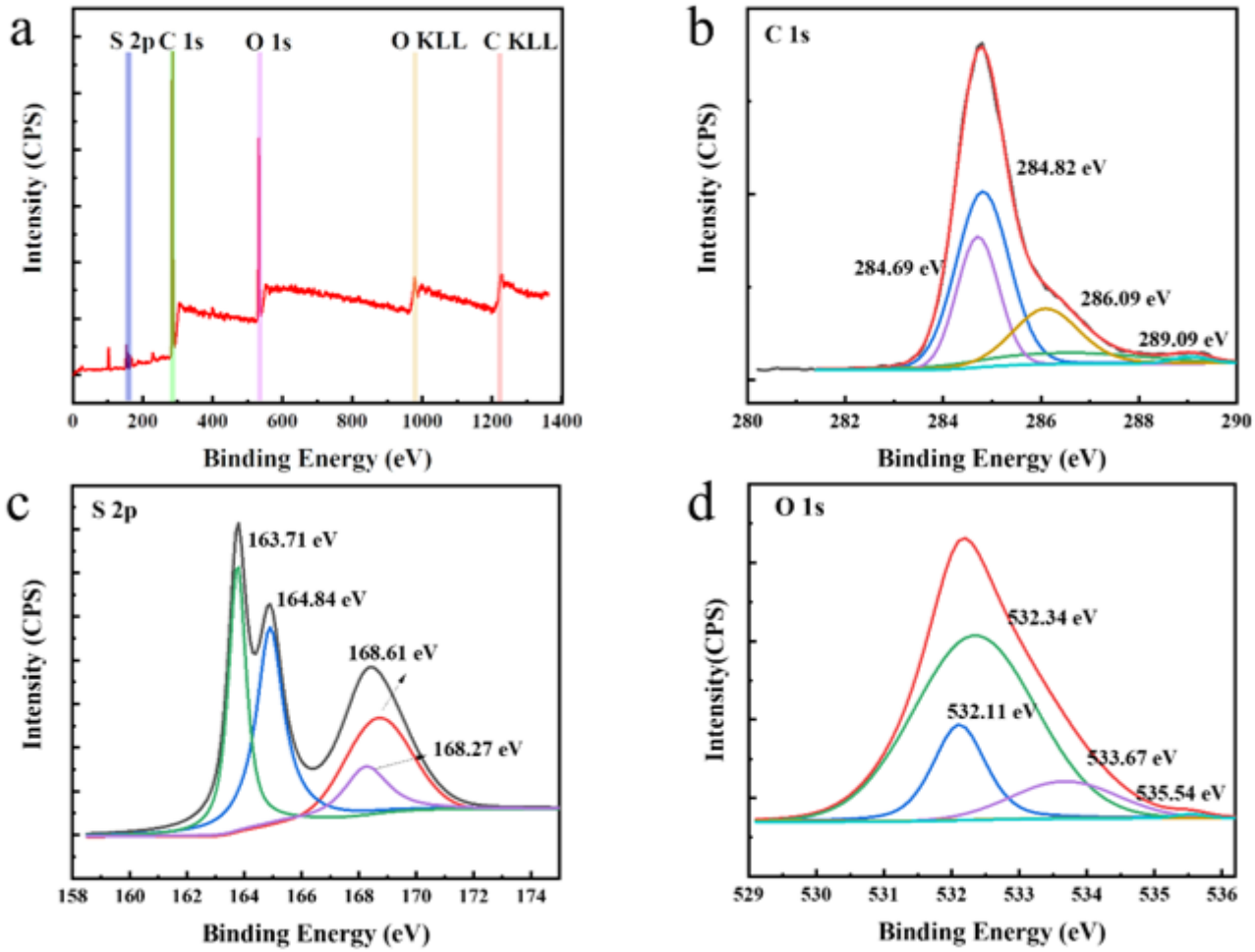

Figure 3

(a)XPS survey spectra of 15 wt% PCPP film. (b-d) XPS spectra of C 1s, S 2p, O 1s of 15 wt% PCPP film.

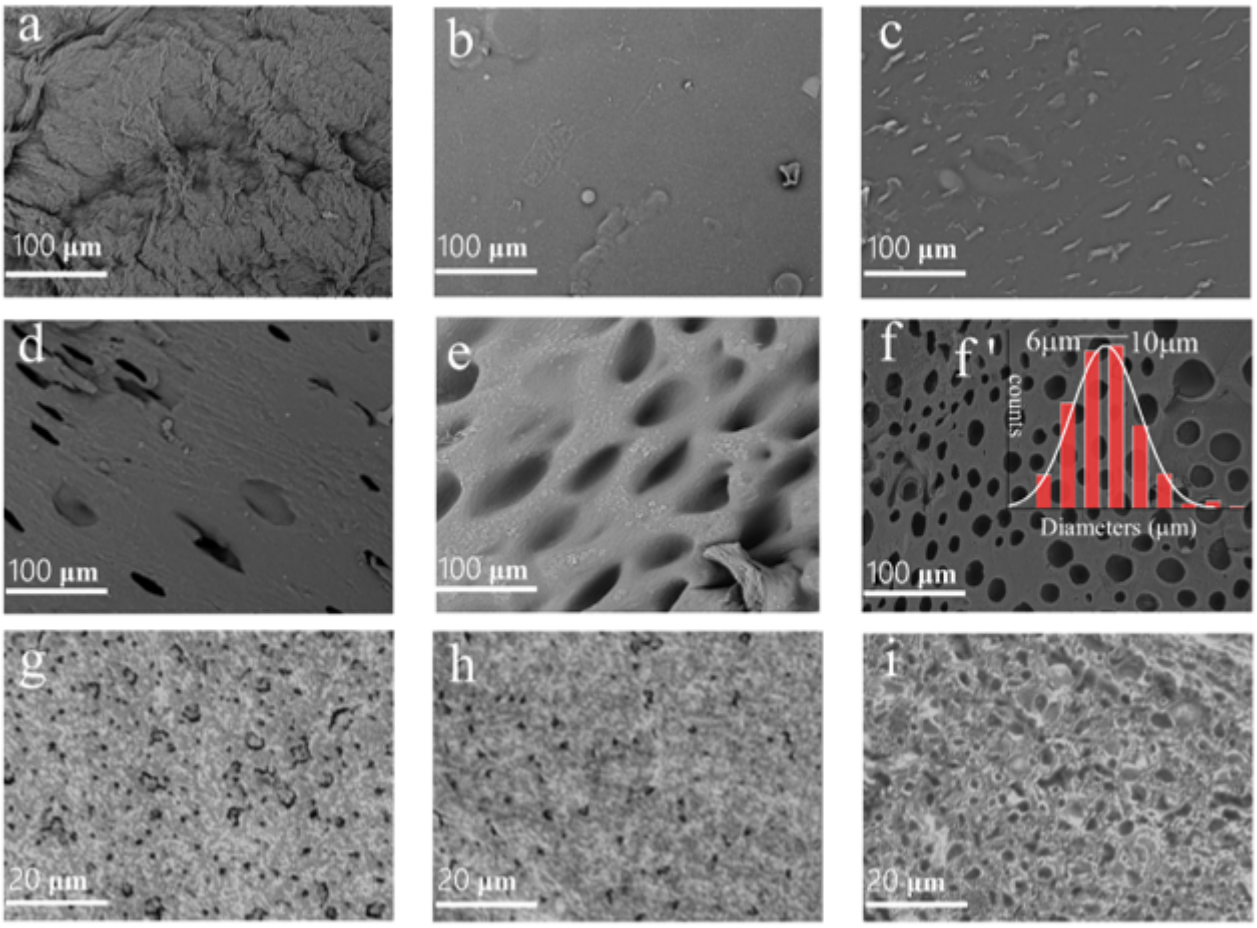

Figure 4

(a-i) SEM images of films. (a) CEL film. (b) PVA/CEL film. (c) PVA/CEL/EDOT film. (d) coagulation bath-water-10 wt% PCPP film. (e) coagulation bath-water-12 wt% PCPP film. (f) coagulation bath-water-15 wt% PCPP film (f´) Diameters distribution of 15 wt% PCPP film. (g) coagulation bath-ethanol-10 wt% PCPP film. (h) coagulation bath-ethanol-12 wt% PCPP film. (i) coagulation bath-ethanol-15 wt% PCPP film.

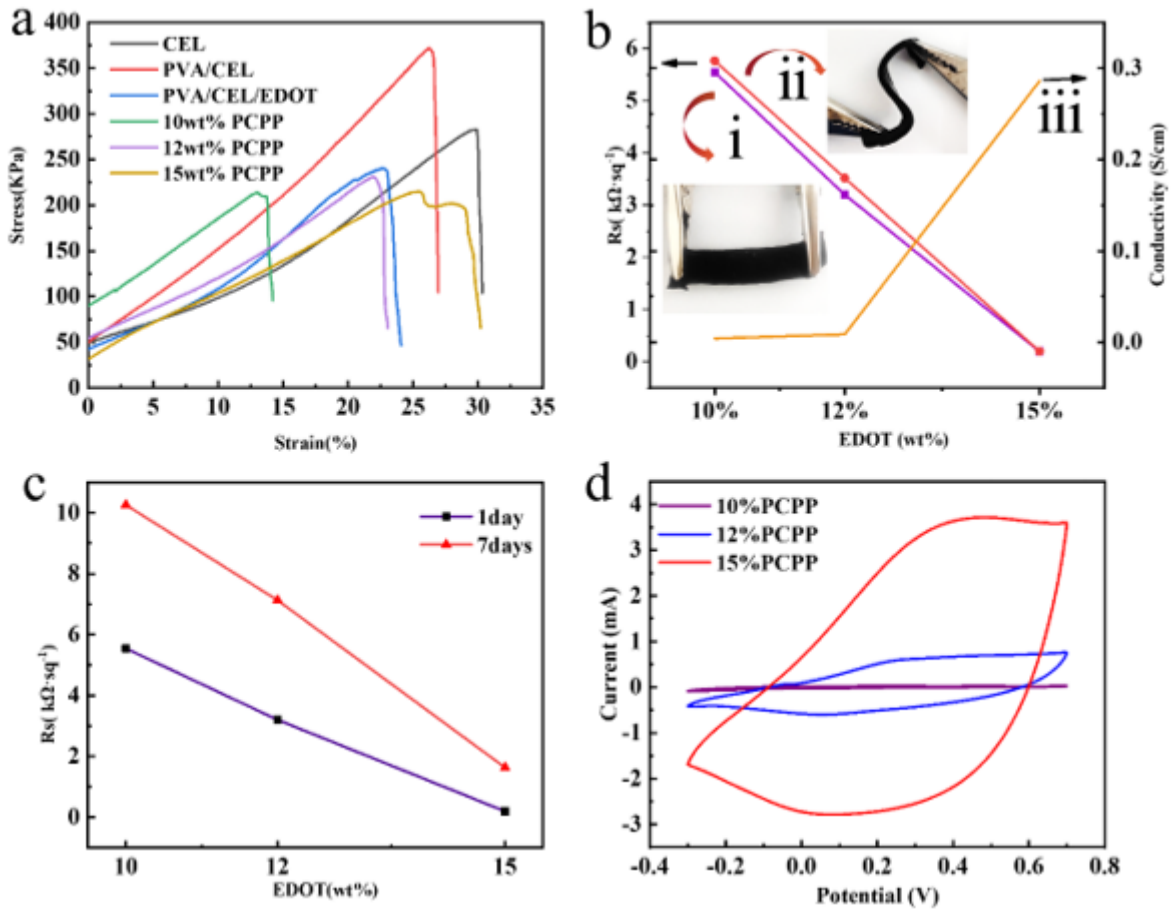

Figure 5

(a) stress-strain curves of the PCPP films. (b) Sheet resistance and conductivity of the PCPP films as a function of the EDOT content. curve is the sheet resistance under normal conditions. curve is the sheet resistance in the case of curling. curve is the conductivity of the PCPP films. (c)The resistance of PCPP films on day 1 and 7. (d) CV curves record at 0.01 Vs-1.

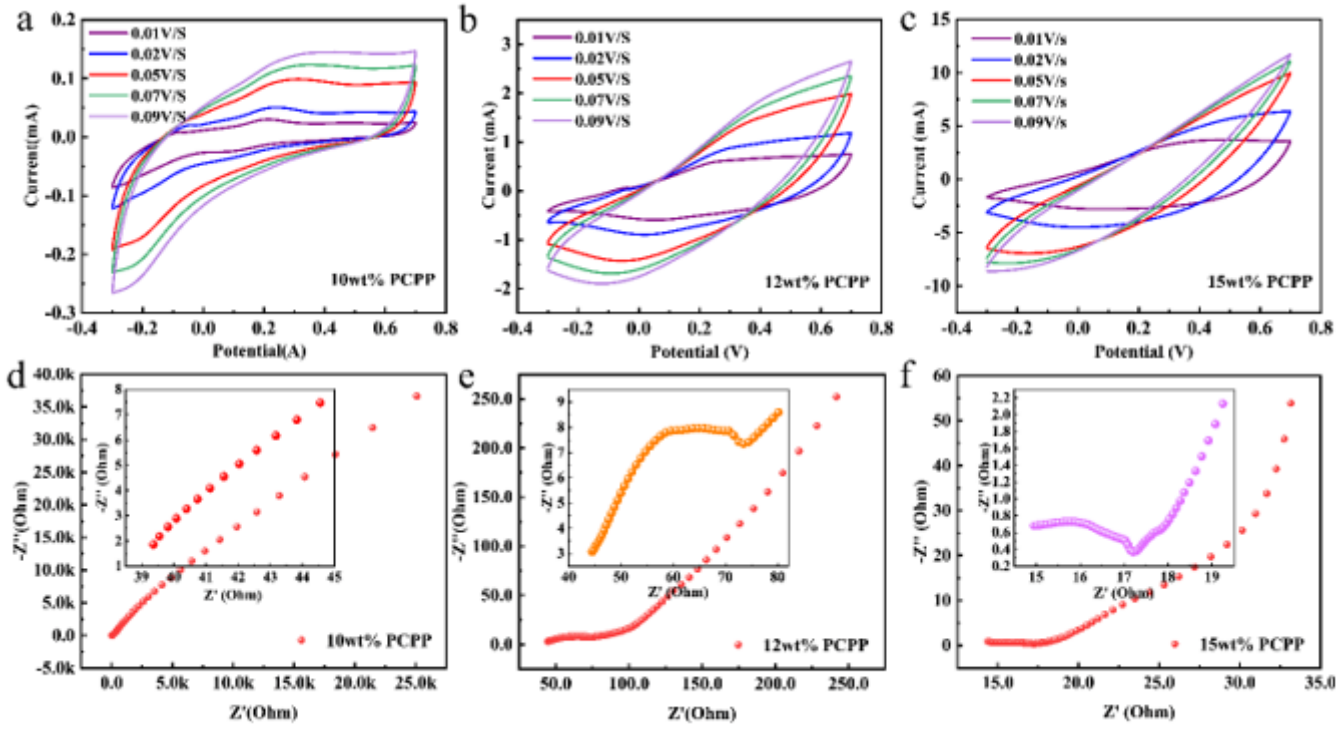

Figure 6

(a-c) CV curves of the 10 wt%, 12 wt%, 15 wt% PCPPs at scan rates of 0.01-0.09Vs-1. (d-f) Nyquist plot of 10 wt%, 12 wt%, 15 wt% PCPP electrodes. Inset: a magnified of the high-frequency region.

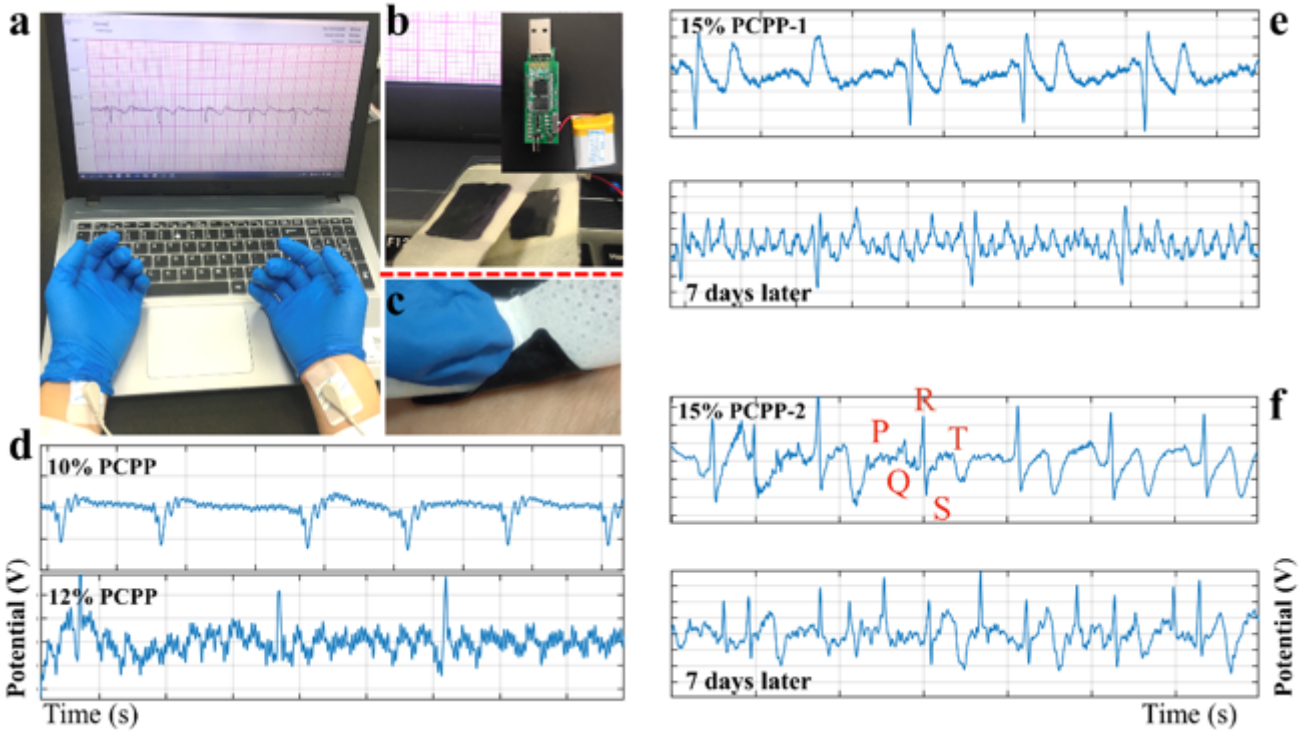

Figure 7

(a) Photograph of PC software for real-time monitoring of ECG curve. (b) Photograph of 15 wt% PCPP electrode and analog front end circuitry in the top right. (c) Photograph of contacting with the skin without any irritation. (d) ECG spectrum obtained from 10 wt% and 12 wt% PCPP electrodes. (e-f) ECG spectra of two volunteers obtained from 15 wt% PCPP electrode and ECG spectra obtained after 7 days.

Supplementary Files

This is a list of supplementary files associated with this preprint. Click to download.

- Graphicalabstract.docx
- SupplementaryInformation.docx